

# Early-stage roughening of the polymer-polymer interface approaching the glass transition temperature by real-time neutron reflection

C. Carelli,<sup>1,\*</sup> A. M. Higgins,<sup>2,†</sup> R. A. L. Jones,<sup>2</sup> and M. Sferrazza<sup>3,‡</sup>

<sup>1</sup>*Department of Physics, University of Surrey, Guildford, United Kingdom*

<sup>2</sup>*Department of Physics and Astronomy, University of Sheffield, Sheffield, United Kingdom*

<sup>3</sup>*Département de Physique, Université Libre de Bruxelles, Boulevard du Triomphe, CP223, Bruxelles, Belgium*

(Received 13 March 2006; published 29 June 2006)

The early-stage roughening of the interface between thin deuterated poly(methyl methacrylate) (d-PMMA) layers on thick polystyrene (PS) films was studied as a function of the temperature using real-time specular neutron reflectivity. By measuring the growth of the interface roughness as a precursor of the dewetting, the characteristic time constant of the early stages of the process was studied as a function of the temperature approaching the glass transition temperature ( $T_g$ ) of the two polymers from above and compared with the prediction of the growth of the interface by the spinodal process. Both solid and liquid regimes were probed, in which the viscosity of the thin film or the substrate dominates respectively. The characteristic growth time of the process also depends on the upper film thickness to a power of 5 or 6 in the solid or liquid regimes, respectively, as predicted by the theory of spinodal dewetting.

DOI: [10.1103/PhysRevE.73.061804](https://doi.org/10.1103/PhysRevE.73.061804)

PACS number(s): 82.35.Rs, 68.08.-p, 68.55.-a

## I. INTRODUCTION

The roughening of the surface and interface of a thin polymer film as the precursor process of the dewetting is an interesting process in polymer physics related to the growth of capillary waves at the surface and interface: during this process, at the early stages, the interface and surface grow with a characteristic time that is related mainly to the viscosities and thicknesses of the films [1–5]. While the final stage of the spinodal dewetting process, where a thin liquid film breaks up forming the classic network pattern has been extensively studied using imaging techniques, such as atomic force microscopy and optical microscopy ([6–10] to cite a few), the study of the early stage of the growth of the interface has been less studied, mainly because being at a burred interface presents an experimental challenge. Neutron reflectivity has proved essential to investigate this process [4,11]. In the case of a thin polymer film on a polymer substrate, solid and liquid regimes are predicted depending on the relative viscosities of the layers, with different time constants for the film breakup: a solid regime is where the viscosity of substrate is much greater than the one of the top layer and the process is governed by the viscosity of the top thin film, where in the liquid regime the viscosity of the substrate dominates [1–3]. These regimes for a polymer-polymer system could be probed for the same system by selecting appropriate molecular weights (MW) of the polymers and annealing temperature. In our previous studies on the dewetting of a thin polymer film on a polymer substrate, we have investigated a thin poly(methyl methacrylate) (PMMA) film on a

thick polystyrene (PS) layer. We have observed the growth of the interface and surface, associated to the unstable growth of capillary waves, by both specular and off-specular neutron scattering at the early stages [4,11], and the characteristic pattern of the spinodal dewetting, with a length of the order of microns, by atomic force microscopy (AFM) at the late stages of the process [12]. In particular, by measuring the growth of the interface at the early stage, we were able to use this process to probe the scaling of the top PMMA thin film viscosity with temperature and molecular weight (MW) and we have found that for the temperatures and MW used, the scaling reflects bulk behavior. In those systems we were in the condition of the solid regime, where the dewetting is mainly related to the viscosity of the top thin layer [11]. To gain more insight on the observed instability of the PMMA-PS system, we have studied the early stage of the roughening of the interface by performing various neutron reflectivity experiments on the same combination of MW and thicknesses of the polymers using different annealing temperature from 164 °C to 110 °C approaching the glass transition of both polymers. Different regions of the growth rate of the interface were observed as a function of the temperature: we observe a transition from the solid regime to the liquid regime for the characteristic rise time of the interface when the annealing temperature was decreased. Considering the slippage length at the interface between the two polymers, the results were well described by the theory of spinodal dewetting. The characteristic growth time of the process also depends on the upper film thickness with to a power of 5 in the solid regime and 6 in the liquid one.

## II. EXPERIMENTAL SECTION

Systems were prepared by first spin coating polystyrene (PS) (molecular weight  $\sim 1.9$  M g/mol) onto single crystal silicon substrates from toluene solution. The deuterated poly(methyl methacrylate) (d-PMMA) layer (molecular weight = 155 K g/mol or 120 K g/mol) were first spun from

\*Present address: Ecole Supérieure de Physique et Chimie Industrielles (ESPCI), Paris, France.

†Present address: School of Engineering, University of Wales Swansea, Singleton Park, Swansea, UK.

‡To whom correspondence should be addressed. Email address: msferraz@ulb.ac.be

TABLE I. Summary of the MW, thickness ( $t$ ), and temperature (Temp.) of the various PS and PMMA systems.

MW <sub>PMMA</sub> (g/mol)	MW <sub>PS</sub> (g/mol)	$t_{PMMA}$ (Å)	$t_{PS}$ (Å)	Temp. (°C)
$1.55 \times 10^5$	$1.98 \times 10^6$	82	1501	110
$1.55 \times 10^5$	$1.98 \times 10^6$	81	1550	120
$1.20 \times 10^5$	$1.93 \times 10^6$	81	1488	135
$1.20 \times 10^5$	$1.93 \times 10^6$	77	1480	140
$1.20 \times 10^5$	$1.93 \times 10^6$	76	1489	146
$1.20 \times 10^5$	$1.93 \times 10^6$	77	1467	152
$1.20 \times 10^5$	$1.93 \times 10^6$	108	1502	148
$1.20 \times 10^5$	$1.93 \times 10^6$	106	1510	152
$1.20 \times 10^5$	$1.93 \times 10^6$	111	1514	155
$1.20 \times 10^5$	$1.93 \times 10^6$	105	1495	158
$1.20 \times 10^5$	$1.93 \times 10^6$	112	1561	164

toluene solution onto glass slides and the resulting films were then floated in water and deposited on top of the PS layers. All the polymers were obtained from Polymer Laboratories (UK) and had MW/Mn=1.1 or less. The films were then annealed for some time at temperature well below the glass transition to allow the evaporation of the solvent and relaxation of the polymers to take place. In order to study the dynamic of the dewetting process of the PS by a PMMA thin film, samples have been annealed at different temperatures above  $T_g$ , and specular neutron reflectivity has been measured.

The earlier growth of the interface and surface roughnesses was measured with real-time specular neutron reflectivity. The reflectivity curves were acquired by selecting a restricted range of  $q$  and measuring the curves *in situ* every  $\sim 10$  min. Neutron reflectivity experiments were performed on reflectometers in different facilities: SURF at the Rutherford Appleton Laboratory (UK), D17 at the Institut Max Von Lau-Paul Langevin (France), and V6 at the Hein Meitner Institut (Germany). On SURF and D17, we measured *in situ* neutron reflectivity: after measuring the specular reflectivity over the full  $q$  range before annealing, the samples were annealed *in situ*, in the neutron beam, at a fixed temperature. We followed the dewetting process by continuously measuring the reflectivity at one angle: this angle was chosen in order to follow the decay of the fringe characteristic of the

TABLE II. Summary of the MW, thickness, and temperature of the different PS and PMMA systems.

MW <sub>PMMA</sub> (g/mol)	MW <sub>PS</sub> (g/mol)	$t_{PMMA}$ (Å)	$t_{PS}$ (Å)	Temp. (°C)
$1.55 \times 10^5$	$1.98 \times 10^6$	53	1518	120
$1.55 \times 10^5$	$1.98 \times 10^6$	64	1550	120
$1.55 \times 10^5$	$1.98 \times 10^6$	81	1499	120
$1.55 \times 10^5$	$1.98 \times 10^6$	81	1488	135
$1.55 \times 10^5$	$1.98 \times 10^6$	95	1515	135
$1.55 \times 10^5$	$1.98 \times 10^6$	125	1502	135

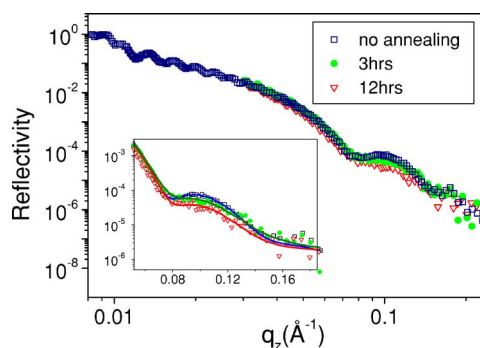


FIG. 1. (Color online) *In situ* reflectivity curves for an 80 Å d-PMMA layer on a PS substrate of 1500 Å annealed at 110 °C for different annealing times reported in the figure. As the annealing time increases the fringe related to the thickness of the d-PMMA layer decreases in intensity. The lines are the fit obtained using the surface and interface roughness as variable parameters (see text for details). Data from ILL (Grenoble).

interference of the front and back of the d-PMMA film thickness. The resolution was adapted to reduce the time required for each run and be able to collect a large number of data points: on D17 it was 6%, while on SURF it was 8%. On the reflectometer V6 at HMI, we performed specular neutron reflectivity experiments on series of samples previously annealed in a vacuum oven: we followed the growth of the interface by measuring the reflectivity over the full  $q$  range on samples annealed at the same temperature for different length time. The resolution was 6%.

As for our previous experiments [4,11], we kept the MW of the PS at 1.98 M or 1.93 M g/mol and the MW of the d-PMMA at 155 K or 120 K g/mol. Different series of samples have been measured. For two different values of d-PMMA thickness (80 Å and 110 Å) the dewetting process has been studied as a function of the annealing temperature, in the range 110–164 °C. Table I shows the MW and the film thicknesses of the various systems investigated.

In other series of samples, the PMMA thickness has been changed while the annealing temperature was fixed (120 °C and 135 °C). The thickness of the bottom layer of PS was fixed for all the samples at about 1500 Å. Table II summarizes the systems studied.

The film thickness of both layers, as well as the silicon oxide layer on the silicon substrate, were measured by ellipsometry prior the final preparation of the sample. Figure 1 shows as an example a set of *in situ* reflectivity measurements for the 80 Å d-PMMA layer, respectively, on PS substrates annealed at a temperature of 110 °C. The prominent fringe is the result of interference between the front and the back of the d-PMMA layer, while the high frequency fringes are connected to the PS thickness. During the annealing the visibility of the fringe is reduced as the roughnesses present at surface and interface are increasing with the annealing time.

### III. RESULTS

The measured neutron reflectivity profiles were analysed using the multilayers model *silicon substrate-silicon oxide-*

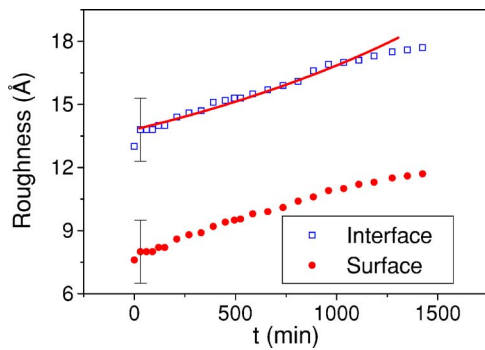


FIG. 2. (Color online) Surface and interface roughness as a function of the annealing time for a PMMA layer of 80 Å deposited on a PS substrate of thickness 1500 Å annealed at 110 °C. The error on the roughness is shown on the first point only for clarity. The line is an example of the fit obtained using Eq. (1).

*PS-deuterated PMMA-air.* The silicon oxide layer thickness has been fixed to the value measured with ellipsometry, while the PS and the PMMA film thickness have been determined from the fringes in the reflectivity curves (the value obtained by the fit were in good agreement with the value obtained by ellipsometry). During the fit, the roughness of the silicon oxide layer has been fixed to 5 Å, as we have measured with neutron reflectivity on uncoated substrates [4,11]. The values of the scattering length densities used for the two polymers were respectively  $6.7 \times 10^{-6} \text{ \AA}^{-2}$  for d-PMMA and  $1.4 \times 10^{-6} \text{ \AA}^{-2}$  for PS. The reflectivity profiles measured during the annealing process have been fitted using two variable parameters, the PS-d-PMMA interfacial roughness and the d-PMMA surface roughness. For all the samples an immediate increase in both the roughnesses was observed, which may be due to the broadening of the intrinsic width of the interfacial region. This is followed by a gradual increase in the roughness at surface and interface that represents the early stage of the interfacial instabilities precursors of the dewetting. The development of the surface and interface roughness for 80 Å PMMA film on a PS layer annealed at 110 °C is shown in Fig. 2. Due to the high viscosity of the polymers at this temperature, close to the glass transition

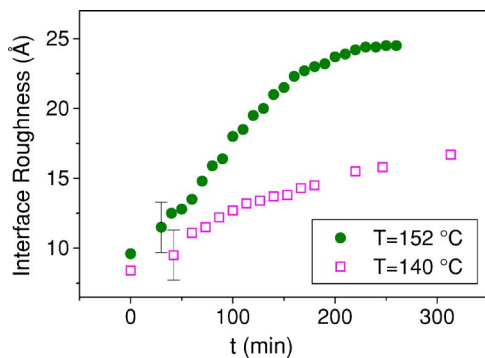


FIG. 3. (Color online) Interface roughness as a function of the annealing time for 80 Å PMMA films deposited on a PS substrate of thickness 1500 Å. The annealing temperatures were 140 °C (open square) and 152 °C (full symbol). The error on the roughness is shown on the first point only for clarity.

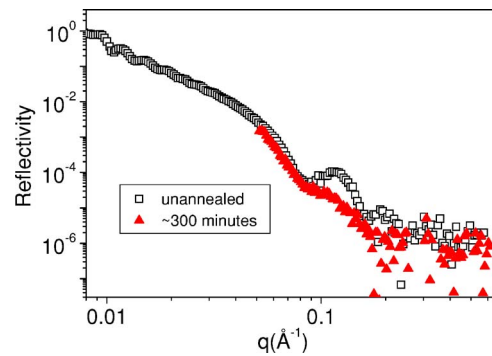


FIG. 4. (Color online) Reflectivity at the beginning and after 300 min of annealing for 80 Å PMMA films deposited on a PS substrate of thickness 1500 Å. The annealing temperatures were 146 °C. Data from CRISP (RAL)

temperature, the growth is slow and both surface and interface roughness present similar growth.

Figure 3 shows instead the earlier growth of the PS/PMMA interface roughness for PMMA films of 80 Å annealed at different temperatures, 140 °C and 152 °C. For both samples, the roughness increases by a significant amount, but the roughening time is lower for the higher temperature. The dewetting of the top layer is evident in Fig. 4 where we show the reflectivity for the final stage of the process in comparison to the reflectivity at the beginning: the fringe associated to the thin PMMA layer disappeared.

From Figs. 2 and 3, it is clear that the earlier growth of the interface is characterized by a well-defined time scale that depends on the PMMA thickness and on the annealing temperature. This is the reason why it is very crucial to prepare samples with similar thickness. To determine the characteristic earlier roughening time  $\tau$  for the different systems studied, the growth of the roughness in the early stage of the process has been fitted using the expression introduced in our previous paper [11]:

$$\sigma(t) = \sqrt{A + \frac{Be^{t/\tau} \text{erf}(\sqrt{t/\tau})}{\sqrt{t/\tau}}}, \quad (1)$$

where in the square root expression the first term represents waves vectors of capillary waves that do not grow in amplitude while the second term represents those that grow in amplitude with the annealing time  $t$ . This relation was obtained by considering that the growth in capillary roughness is given by  $\sigma_2(t) = (\zeta(t) - e)^2$ , with  $e$  the thickness of the thin film and  $\zeta = e + u_q e^{iqt} e^{t/\tau}$  representing the perturbations obeying the dispersion relation for  $\tau_q$ . By integrating the roughness above over all wave vector, Eq. (1) was obtained [11].

Figure 5 shows the characteristic time  $\tau$ , obtained from the fits, as a function of the annealing time for two different thicknesses of the PMMA film, 80 Å and 110 Å, together with the results we have obtained previously for the 137 Å [11].



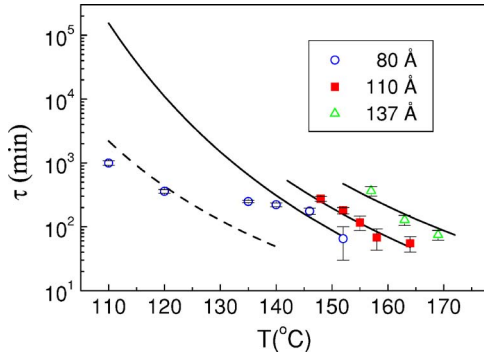


FIG. 5. (Color online) Characteristic growth time of dewetting  $\tau$  as a function of the temperature of annealing for 80 Å (open circle) and 110 Å (full square) and 137 Å (taken from [11]) (triangle) from d-PMMA films. The continuous lines represent the theoretical prediction divided by a scale factor of the order of  $10^4$  in the solid-substrate regime (line) and in the liquid-substrate regime (dotted line) (see text for details). All the data points corresponding to 110 Å were obtained from *in situ* experiments at ISIS (RAL), as well as for 80 Å except the data points for  $T=110^\circ$  and  $120^\circ$  measured from *in situ* experiments at ILL. The data point for  $T=135^\circ$  was measured using the all  $q$  range on V6 (Berlin).

#### IV. DISCUSSION

From Fig. 5 we can observe that for higher temperatures the dewetting process is very fast, while the characteristic growth time increases for lower temperatures. The dewetting time also depends strongly on the thickness of the PMMA layer, and thicker layer presents longer time scale. To analyze these results more quantitatively, it is important to define the regime of the substrate. For a liquid film of viscosity  $\eta_F$  on a substrate of viscosity  $\eta_S$ , the crossover from a liquid to a solid substrate regime should occur when

$$\eta_S > (\eta_F / \Theta_E), \quad (2)$$

where  $\Theta_E$  is the Neuman equilibrium contact [2], determined by the values of the interfacial tension between PS and PMMA and the surface tensions of the two polymers [13]. Since the angle  $\Theta_E$  is of the order of 1 radian (1.28 has been calculated for  $T=150^\circ\text{C}$  [14]), an estimation of the viscosity of the two polymers as a function of the temperature is required to probe the regime of the PS substrate. To predict the dependence of the viscosity  $\eta$  on the temperature, the William-Landel-Ferry (WLF) equation has been used [15],

$$\eta(T) = \eta_0 \exp\left(\frac{-C_1(T-T_0)}{C_2 + (T-T_0)}\right) \quad (3)$$

where  $\eta_0$  is the zero shear rate viscosity, i.e., the value of the viscosity at a reference temperature  $T_0$ ,  $C_1$  and  $C_2$  are constants that depend on the reference temperature chosen, and  $T$  is the temperature.

To estimate the PMMA viscosity  $\eta_{PMMA}$ , two different reference temperatures have been used in Eq. (3). Above  $160^\circ\text{C}$  the reference temperature was  $190^\circ\text{C}$  and the relative values of the constants  $C_1$  and  $C_2$  were respectively  $C_1=8.9$  and  $C_2=176$  [16]. The zero shear rate viscosity at  $190^\circ\text{C}$  found in the literature for PMMA of molecular

weight  $MW=10^5$  g/mol is  $\eta_0=1.04 \times 10^6$  Pa s, and it has been corrected with the equation  $\eta \propto MW^{3.4}$  to obtain the value correspondent to the molecular weights used ( $MW=1.20 \times 10^5$  g/mol and  $MW=1.55 \times 10^5$  g/mol).

For temperatures below  $160^\circ\text{C}$ , the glass transition temperature for PMMA ( $T_g=105^\circ\text{C}$ ) has been used as a reference temperature with  $C_1=20.9$  and  $C_2=58$  [17]: the viscosity at  $T_g$  has been determined from Eq. (3) using the value previously determined for  $\eta(T)$  at  $T=160^\circ\text{C}$ . The values obtained for the PMMA viscosity at the glass transition following this procedure are  $\eta(T_g)=3.8 \times 10^{11}$  Pa s for  $MW=1.20 \times 10^5$  g/mol and  $\eta(T_g)=9.1 \times 10^{11}$  Pa s for  $MW=1.55 \times 10^5$  g/mol.

To calculate the PS viscosity,  $\eta_{PS}$  the WLF equation has been used considering the glass transition as a reference temperature (for PS  $100^\circ\text{C}$ ) and the values  $C_1=13.7$ ,  $C_2=50.0$  for the two constants [17]. To determine the zero shear rate viscosity  $\eta_0$  at the glass transition, the value of viscosity  $\eta_0=3.4 \times 10^4$  Pa s for  $MW=2.4 \times 10^5$  g/mol at  $183^\circ\text{C}$  [18] has been used. The value calculated for  $\eta_T$  is  $1.9 \times 10^{11}$  Pa s for  $MW=1.9 \times 10^6$  g/mol. These values of viscosity are consistent with other values found in the literature [19]. A comparison between the values obtained for the viscosities of PS and PMMA as a function of the temperature shows that for both the molecular weights of the PMMA used, there is a crossover from a liquid to a solid substrate when the temperature is increased. In the case of PMMA with molecular weight  $1.20 \times 10^5$  g/mol it should occur at about  $122^\circ\text{C}$ , while for  $MW=1.55 \times 10^5$  g/mol it should be at about  $129^\circ\text{C}$ .

It is therefore possible to define regions with different regimes: for temperatures lower than  $\sim 120^\circ\text{C}$  the substrate behaves like a liquid, while for temperatures well above the crossover the substrate can be considered as a solid.

In the solid substrate regime assuming no slippage at polymer-polymer interface, the characteristic growth time  $\tau_{SOL}$  is directly proportional to the viscosity of PMMA,  $\eta_{PMMA}$ , following the equation [1,2]

$$\tau_{SOL} = 3 \eta_{PMMA} / (2d^3 \gamma q_m^4), \quad (4)$$

where  $d$  is the PMMA thickness,  $\gamma$  is the interfacial tension and  $q_m$  is the wave vector of the capillary waves that grows faster. The values of the viscosity estimated for PS and PMMA as a function of the temperature have been used in Eq. (4) to compare the experimental  $\tau$  with the theory. The PS/PMMA interfacial tension used is 2 mN/m, where the temperature dependence, that does not influence significantly the results, has been ignored [20].

The characteristic wave vector  $q_m$  can be estimated using our off-specular measurements on the same sample structure with similar thickness [4]: using  $q_m=2\pi/\lambda_m$ , where  $\lambda_m$  is the wavelength of the capillary waves that growth faster, we estimate  $q_m \sim 7 \times 10^6$  m $^{-1}$  for the PMMA layer of 80 Å and  $q_m \sim 4 \times 10^6$  m $^{-1}$  for the PMMA layer of 110 Å [4].

The experimental values found for  $\tau_{SOL}$  are approximately four orders of magnitude lower than the theoretical bulk value.

This factor may be explained assuming slippage at polymer-polymer interface. In this case it is possible to define an extrapolation length  $b$  that measures the slippage, given by the ratio between the viscosity and the friction coefficient  $k$ ,  $b = \eta/k$  [21]. Assuming slippage, Eq. (4) can be written as

$$\tau_{SOL} = 3\eta_{PMMA}/[2d^2(d+3b)\gamma q_m^4]. \quad (5)$$

If Eq. (5) is used to determine the extrapolation length from the experimental data, in order to obtain a good agreement with the experimental results, as shown in Fig. 5, a value of  $b$  is around  $15 \mu\text{m}$  for the  $80 \text{ \AA}$  system, and around  $30 \mu\text{m}$  for the  $110 \text{ \AA}$  are needed (the solid lines in Fig. 5 represent the estimated values using these values of  $b$ ).

The slippage length  $b$ , of the order of tens of microns is similar to the ones observed in other polymeric systems [22]. A simple upper bound for  $b$  is given by the following equation [23]:

$$b = \frac{\eta a^2}{\epsilon}, \quad (6)$$

where  $\eta$  is the viscosity,  $a$  is the characteristic polymer length (the statistical segment length), and  $\epsilon$  is the monomeric friction coefficient.  $\epsilon$  can be expressed in terms of the viscosity as [23]

$$\epsilon = \frac{36\eta\rho}{a^2 N^2}, \quad (7)$$

where  $\rho$  is the volume occupied by a molecule and  $N$  is the degree of polymerization. Thus Eq. (6) becomes

$$b = \frac{a^4 N^2}{36\rho}. \quad (8)$$

Using a characteristic length  $a$  of  $7 \text{ \AA}$  [4], a volume per molecule  $\rho$  of  $174 \text{ \AA}^3$  [4] and  $\sim 1200$  for the degree of polymerization  $N$  of PMMA, the estimated upper limit value for the extrapolation length  $b$  is  $55 \mu\text{m}$ , consistent with the estimated values of around  $15\text{--}30 \mu\text{m}$  extracted from our experimental results.

The dependence of the time constant of the dewetting process on the thickness of the PMMA layer has also been analyzed. The theory in the solid regime predicts for  $\tau$  a strong dependence on the PMMA thickness. In fact considering that from the theory  $q_m$  is proportional to  $1/d^2$  [2,4], Eq. (4) give  $\tau_{SOL} \propto d^5$  [1,2]. In Fig. 6 the ratio  $\tau_{SOL}/d^5$  has been plotted for samples with different PMMA thicknesses. For temperatures higher than  $140 \text{ }^\circ\text{C}$  the data collapse to the same values suggesting indeed a dependence on the fifth power on the PMMA thickness.

Below  $145 \text{ }^\circ\text{C}$  the experimental data show a slow down on the characteristic growth time, probably connected to the fact that in this region the PS and PMMA viscosities are of the same order of magnitude: the resulting characteristic growth time is then given by a combination of both the viscosities.

For temperatures below  $135 \text{ }^\circ\text{C}$  (liquid regime), the characteristic growth time  $\tau$  for the dewetting of the PMMA thin film on the liquid PS substrate depends on the PS viscosity

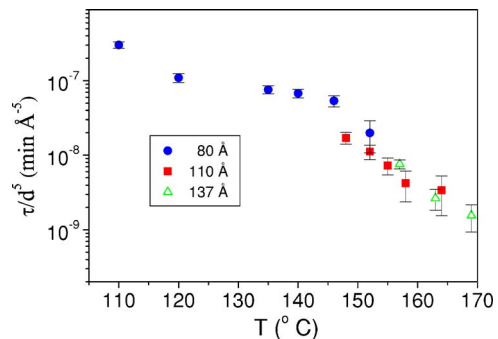


FIG. 6. (Color online) Characteristic growth time of dewetting  $\tau$  divided by the  $d^5$  ( $d$  is the PMMA thickness) as a function of the temperature of annealing for  $80 \text{ \AA}$ ,  $110 \text{ \AA}$ , and  $137 \text{ \AA}$  [11] PMMA films on PS substrates (see text for details).

$\eta_S$ . Assuming slippage,  $\tau_{LIQ}$  is given by the following equation [2]:

$$\tau_{LIQ} = 3\eta_S/[2d(d+3b)\gamma q_m^4 D], \quad (9)$$

where  $D$  is the thickness of the PS substrate. Using the same slippage factor found in the solid-substrate regime, there is a reasonable agreement between the calculated values and the experimental results, as shown by the dotted line in Fig. 5. In the transition from solid to liquid regime the dependence of the characteristic growth time on the thickness of the top layer should increase. For a thin layer on a liquid substrate the theory predicts for  $\tau$  a dependence on the sixth power of the thin film thickness,  $\tau_{LIQ} \propto d^6$  [1,2]. In Fig. 7 the experimental data obtained for  $\tau$  as a function of the PMMA thickness for two fixed annealing temperatures are compared with the theoretical prediction.

The data were fitted using equation  $\tau = 3\pi^2 \eta_{PS} \gamma d^6 / (2A^2 D)$ , where the theoretical values for the viscosities, the interfacial tension, the Hamaker constant  $A$ , and the thickness of the bottom layer were inserted in the equation and just the power  $x$  of the exponent of  $d^x$  was fitted. With this limited set of data in the liquid substrate regime, we obtained a dependence on the thickness of  $6.1 \pm 0.3$  and  $5.8 \pm 0.3$  for

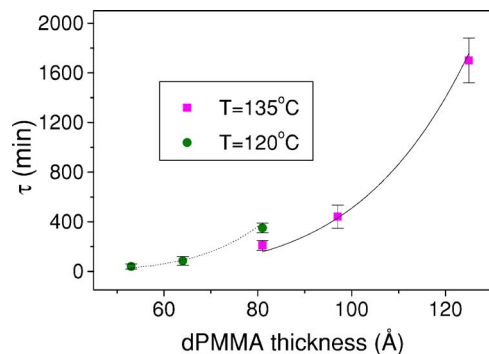


FIG. 7. (Color online) Characteristic growth time  $\tau$  as a function of the thickness of the PMMA film for two different annealing temperatures:  $120 \text{ }^\circ\text{C}$  and  $135 \text{ }^\circ\text{C}$ . At  $120 \text{ }^\circ\text{C}$  the fit shows agreement with the theoretical prediction for the liquid regime ( $\tau \sim d^6$ ).

the 120 °C and 135 °C cases, respectively, in good agreement to the value predicted for the liquid regime of 6 [1,2].

## V. CONCLUSIONS

We have studied the early stages of the roughening of the interface as the precursor process of the interfacial instabilities of a thin polymer film on a polymer substrate with real-time neutron reflectivity. By following the growth of the interface as a function of the time at different annealing time approaching  $T_g$  from above, we were able to extract the characteristic rise time of the instability and to compare it with

the prediction of the spinodal dewetting process. Both solid and liquid regimes, where the viscosity of the top or bottom layer dominates respectively, were characterized. The characteristic growth time depends also on the fifth power of the top thin layer in the solid regime and on the sixth power in the liquid regime as predicted by the theory.

## ACKNOWLEDGMENTS

We would like to thank R. Cubitt (ILL), R. Krastev (BENSC), and J. Webster (RAL) for their help during the neutrons reflectivity experiments.

- 
- [1] F. Brochard-Wyart *et al.*, *Can. J. Phys.* **68**, 1084 (1990).  
 [2] F. Brochard-Wyart *et al.*, *Langmuir* **9**, 3682 (1993).  
 [3] A. Vrij, *Discuss. Faraday Soc.* **42**, 23 (1966).  
 [4] M. Sferrazza *et al.*, *Phys. Rev. Lett.* **81**, 5173 (1998).  
 [5] M. Sferrazza *et al.*, *Philos. Mag. Lett.* **80**, 561 (2000).  
 [6] G. Reiter, *Phys. Rev. Lett.* **68**, 75 (1992).  
 [7] R. Xie *et al.*, *Phys. Rev. Lett.* **81**, 1251 (1998).  
 [8] R. Seeman *et al.*, *J. Phys.: Condens. Matter* **13**, 4925 (2001).  
 [9] G. Kraush., *J. Phys.: Condens. Matter* **9**, 2741 (1997).  
 [10] M. D. Morariu *et al.*, *Phys. Rev. Lett.* **92**, 156102 (2004).  
 [11] A. M. Higgins *et al.*, *Eur. Phys. J. E* **8**, 137 (2002).  
 [12] A. M. Higgins and R. A. L. Jones, *Nature (London)* **404**, 476 (2000).  
 [13] The Neuman angle  $\Theta_E$  is calculated as  $\Theta_E = (-2S/\gamma)^{1/2}$ , where  $\gamma$  is an effective interfacial tension given by  $\gamma = -[(1/\gamma_{PMMA}) + (1/\gamma_{PS/PMMA})]^{-1}$ , and  $S$  is the spreading coefficient defined as  $S = \gamma_{PS} - (\gamma_{PMMA} + \gamma_{PS/PMMA})$  [2].  
 [14] *Polymer Handbook*, 3rd ed. (Wiley, New York, 1989).  
 [15] M. L. Williams, R. F. Landel, and J. D. Ferry, *J. Am. Chem. Soc.* **77**, 3701 (1955).  
 [16] K. Fuchs *et al.*, *Macromolecules* **29**, 5893 (1996).  
 [17] J. D. Ferry, *Viscoelastic Properties of Polymers*, 3rd ed. (Wiley, New York, 1980).  
 [18] R. A. Stratton, *J. Colloid Interface Sci.* **22**, 517 (1966).  
 [19] S. Qu *et al.*, *Macromolecules* **30**, 3640 (1997).  
 [20] T. P. Russell *et al.*, *Macromolecules* **23**, 890 (1990).  
 [21] F. Brochard-Wyart and P. G. de Gennes, *Langmuir* **8**, 3033 (1992).  
 [22] L. Leger *et al.*, *Adv. Colloid Interface Sci.* **94**, 39 (2001).  
 [23] H. R. Brown, *Science* **263**, 1411 (1994).